Proc. Natl. Acad. Sci. USA
Vol. 93, pp. 7053–7058, July 1996
Cell Biology

Brush border myosin-I truncated in the motor domain impairs the distribution and the function of endocytic compartments in an hepatoma cell line

A. DURRBACH*, K. COLLINS†, P. MATSUDAIRA‡, D. LOUVARD*, AND E. COUDRIER*§

*Morphogenèse et Signalisation Cellulaires, Centre National de la Recherche Scientifique, UMR 144, Institut Curie, 26 rue d'Ulm, 75231 Paris Cedex 05 France; †Cold Spring Harbor Laboratory, P.O. Box 100, 1 Bungtown Road, Cold Spring Harbor, NY 11724; and ‡Department of Biology, Massachusetts Institute of Technology, Whitehead Institute for Biomedical Research, 9 Cambridge Center, Cambridge, MA 02142-1479

Communicated by François Jacob, Institut Pasteur, Paris, France, March 7, 1996 (received for review October 13, 1995)

ABSTRACT **Myosins I, a ubiquitous monomeric class of myosins that exhibits actin-based motor properties, are associated with plasma and/or vesicular membranes and have been suggested as players for trafficking events between cell surface and intracellular membranous structures. To investigate the function of myosins I, we have transfected a mouse hepatoma cell line (BWTG3) with cDNAs encoding the chicken brush border myosin-I (BBMI) and two variants truncated in the motor domain. One variant is deleted of the first 446 amino acids and thereby lacks the ATP binding site, whereas the other is deleted of the entire motor domain and lacks the ATP and actin binding sites. We have observed (*i*) that significant amounts of the truncated variants are recovered with membrane fractions after cell fractionation, (*ii*) that they codistribute with a compartment containing α2-macroglobulin internalized for 30 min as determined by fluorescent microscopy, (*iii*) that the production of BBMI-truncated variants impairs the distribution of the acidic compartment and ligands internalized for 30 min, and (*iv*) that the production of the truncated variant containing the actin binding site decreases the rate of α2-macroglobulin degradation whereas the production of the variant lacking the ATP binding site and the actin binding site increases the rate of α2-macroglobulin degradation. These observations indicate that the two truncated variants have a dominant negative effect on the distribution and the function of the endocytic compartments. We propose that an unidentified myosin-I might contribute to the distribution of endocytic compartments in a juxtanuclear position and/or to the regulation of the delivery of ligands to the degradative compartment in BWTG3 cells.**

Myosins I have been characterized first in *Amoeba* and more recently identified in various tissues of vertebrates including brain, liver and adrenal gland (1–8). They have a motor or head domain similar to all the myosins attached to a short carboxy-terminal tail domain. The tail domain of vertebrate myosins I contains two major regions. One region adjacent to the motor domain exhibits IQ motifs providing binding sites for calmodulin. The other region exhibits a sequence motif containing three blocks of conserved residues that to date characterize all myosin-I tails (2). This second region also contains a phospholipid binding site (9). Despite these common features myosins I have been categorized into distinct subclasses based on phylogenetic analysis of their head domain (10). Several subclasses can be expressed in a given cell, and appear to be differentially localized to specific membrane domains (11–14). The difference in the distribution and in the tail structure of the various isoforms might suggest distinct role of these proteins in cell behavior. However, the precise role of myosins I *in vivo* has been investigated only in invertebrate and has been shown to be essential only for two isoforms to date. Antibodies that inhibit the phosphorylation and the function *in vitro* of myosin-IC from *Acanthamoeba castellanii* were able to alter vacuolar contraction *in vivo* (15). Gene disruption of the *myoA* myosin-I in *Aspergillus nidulans* demonstrated an essential role for this myosin-I in secretion and cell growth (16). In contrast, the double disruptions of *myoA* and *myoB* genes, or *myoB* and *myoC* genes in *Dictyostelium*, resulted in viable cells with defects in fluid phase pinicytosis (17, 18).

To study the role of myosin-I in higher eukaryotes we produced variants of a myosin-I, the chicken brush border myosin-I (BBMI), in an hepatoma cell line. We anticipate that the overproduction of variants truncated in the motor domain might have a dominant negative effect on cellular function(s). BBMI from avian and mammalian species, is one of the most extensively studied myosins I in vertebrates. In contrast to two related myosins I, myr1/MIa and myr2/MIb, it exhibits a tissue distribution restricted to the apical domain of enterocytes and proximal tubule cells of kidney (7, 8, 19–22). It is concentrated in the microvilli of these cells where it tethers actin bundles to the plasma membrane and it is also associated with vesicles scattered in the terminal web (21, 23, 24). We show by immunocytochemistry and biochemistry that the production of BBMI-truncated variants, lacking the entire motor domain or the amino-terminal sequence containing the ATP binding site, affect the distribution of the juxta nuclear endocytic compartments and the degradation of α2-macroglobulin. The dominant negative effect of BBMI-truncated variants on the endocytic pathway might suggest the involvement of an unidentified myosin-I in this pathway.

METHODS

Recombinant DNA Constructions. BBMI cDNA (25) (GenBank accession number U04049) containing the complete coding sequence flanked by 258 and 85 bp of the 5′ and 3′ untranslated regions, respectively, was inserted in the *Xba*I and *Eco*RI restriction sites of the eukaryotic expression vector pCB6, which contains the neomycin resistance gene (a kind gift of M. Roth, University of Texas Southwestern Medical Center, Dallas). In this construct, the 5′-end of the BBMI cDNA was located downstream of the cytomegalovirus (CMV) promoter.

To insert the cDNA encoding the BBMI tail (730–1040 aa) in the pCB6 vector, an oligonucleotide (5′-CTGGACATGACGCGTG-3′) containing the 5′ noncoding BBMI bovine sequence (26), an ATG initiation codon, and an *Mlu*I restriction site was subcloned downstream of the CMV promoter into the *Kpn*I–*Eco*RI restriction sites of the vector. Then the recombinant plasmid encoding the tail was obtained by subcloning the cDNA encoding BBMI tail into the *Mlu*I–*Eco*RI restriction sites. The expression of the recombinant plasmid leads to the addition of four amino acids (Thr-Arg-Glu-Phe, TREF) at

The publication costs of this article were defrayed in part by page charge payment. This article must therefore be hereby marked "*advertisement*" in accordance with 18 U.S.C. §1734 solely to indicate this fact.

Abbreviations: BBMI, brush border myosin-I; DTAF, dichlorotriazinyl amino fluorescein; CLSM, confocal laser scanning microscope; TCA, trichloroacetic acid.

§To whom reprint requests should be addressed. e-mail: coudrier@curie.fr.

the amino terminus of tail. Similarly an oligonucleotide (5′-CTGGACATGGAGGCCTGGATCCTGG 3′) containing the 5′ noncoding BBMI bovine sequence (26), an ATG initiation codon, and a *Bam*HI restriction site was subcloned in the same restriction sites of the pCB6 vector prior to subclone the cDNA encoding BBMIΔ446 (446–1040 aa) into the *Bam*HI–*Eco*RI restriction sites.

Cell Culture and Isolation of Stable Transformants. The mouse hepatoma cell line BWTG3 were grown at 37°C under 10% CO_2, in Coon's F12 modified medium (T085-05; Seromed, Berlin) supplemented with 10% fetal calf serum (S0115; Seromed) and penicillin (10 units/ml)/streptomycin (10 mg/ml) (A2213; Seromed) (27). Exponentially growing BWTG3 cells were seeded 24 h before DNA transfer on 5-cm plastic dishes to a cell density of 40%. DNA transfection was performed with lipofectin (8292SA; BRL) and 20 μg of the appropriate DNA following the procedure of Felger *et al.* (28). After 24 h, cells were supplemented with 0.7 mg of Geneticin per ml (066-1811; GIBCO) and permanently grown in this medium. Stable transformants were screened by immunofluorescence staining using the CX-7 antibody directed against the carboxy-terminal domain of chicken BBMI. Two BBMI clones, four BBMIΔ446 clones, and five BBMI tail clones were selected. More than 50% of the cells of these clones produced high levels of proteins, after sodium butyrate treatment [10 mM overnight (29)], as determined by immunofluorescence staining and immunoblotting. Control cells were transfected with the pCB6 vector alone without any insert and grown as described above. They were selected for their ability to grow in the selection medium, whereas all the nontransfected cells died within 15 days in this medium.

Cell Homogenate and Membrane Preparations. Cells were grown 5 days on plastic dishes (10 cm) and incubated overnight in cell culture medium containing 10 mM sodium butyrate before to be scrapped and homogenized by passing the cells in a buffer containing 10 mM Hepes (pH 7.4) and 0.25 M sucrose (HB buffer) through a 22-gauge needle. Unbroken cells and nuclei were removed from the cell homogenate by centrifugation at 1000 × *g* 15 min, and the crude membrane fraction contained in the postnuclear supernatant was loaded in 40.6% sucrose and overlaid successively with 35% sucrose and the HB buffer. After centrifugation for 1 h at 120,000 × *g*, the membrane fraction was collected at the interface of sucrose 35% and the HB buffer, diluted to 6 volumes in Hepes 10 mM (pH 7.4), and centrifuged 45 min at 175,000 × *g*.

Immunofluorescence Microscopy. For immunofluorescence analysis, cells were grown 2 days on coverslips, incubated overnight in cell culture medium containing 10 mM sodium butyrate, fixed with 3% paraformaldehyde and 0.025% glutaraldehyde, permeabilized with phosphate-buffered saline (PBS) containing 0.01% saponin, and analyzed by indirect immunofluorescence. Staining was performed by two sequential incubation steps; cells were first incubated with purified IgG in the case of monoclonal antibodies or affinity purified antibodies in the case of polyclonal antibodies at a concentration of 10 μg/ml. Second, cells were labeled with fluorescent anti-IgG antibodies, conjugated to either lissamine rhodamine B sulfonyl chloride (Molecular Probes) or dichlorotriazinyl amino fluorescein (DTAF) (D2281; Sigma) according to Brandzaeg (30). Fluorescent phalloidin conjugated to either rhodamine (P5157; Sigma) or fluorescein (P5282; Sigma), at 2 units per dish was used to label F actin. To label the acidic compartment with acridine orange, cells were incubated with 2 mM of acridine orange (A-6014; Sigma) diluted in RPMI 1640 medium (041-02402 M; GIBCO) for 30 min, then washed four times with cold PBS and immediately analyzed. Cells were viewed either with a Axiophot microscope (Zeiss), or with a confocal laser scanning microscope (CLSM; Leica).

Endocytosis of Fluorescent α2-Macroglobulin and Transferrin. Iron-loaded human transferrin (T2252; Sigma) and α2-macroglobulin (M7151; Sigma) were coupled either with DTAF or lissamine rhodamine B sulfonyl chloride as described (31). The specific binding of the coupled proteins to the cell surface receptors was determined by competition experiments using 100-fold higher concentration of noncoupled proteins.

Cells were grown 2 days on coverslips, incubated overnight in cell culture medium containing 10 mM sodium butyrate, washed three times with RPMI 1640 medium (041-02402 M; GIBCO) containing 1 mg of bovine serum albumin per ml, followed by a 30-min (twice for 15 min) incubation period with RPMI 1640 medium containing 1 mg of bovine serum albumin per ml at 37°C. The cells were then incubated 30 min at 37°C with DTAF–α2-macroglobulin (20 μg/ml) and/or rhodamine-transferrin (100 nM) in RPMI 1640 medium containing 1 mg of bovine serum albumin per ml. Then cells were washed three times with cold PBS, and either processed for immunofluorescence analysis or fixed 20 min with 3% paraformaldehyde in PBS at 4°C before being observed with a Axiophot microscope (Zeiss) or with the CLSM.

Assay for α2-Macroglobulin Degradation. *Iodination of human α2-macroglobulin.* Human α2-macroglobulin was iodinated by using chloramine T (C 9887; Sigma) as described by Mosher *et al.* (32). The specific activity was 0.43 mCi/mg of protein (1 Ci = 37 GBq). The specificity of binding of radiolabeled α2-macroglobulin was determined by competition experiments with 100-fold higher concentration of nonlabeled α2-macroglobulin (1 mg/ml) that reduced >80% the binding of labeled α2-macroglobulin at 4°C. After iodination, >95% of the radioactivity was precipitable by 10% trichloroacetic acid (TCA).

Endocytosis and degradation at 37°C. ^{125}I-labeled α2-macroglobulin (10 μg/ml) was internalized as described above for the fluorescent α2-macroglobulin in confluent monolayer cultures grown for 2 days in 2.25-cm^2 plates and incubated overnight in cell culture medium containing 10 mM sodium butyrate. After washing, the monolayers were reincubated at 37°C with prewarmed RPMI 1640 medium containing 1 mg of bovine serum albumin per ml. After appropriate chase times, the medium was collected on ice, and undegraded α2-macroglobulin protein was precipitated with 10% TCA. At the end of the experiment, cells were lysed in PBS containing 0.8% Triton X-100. The amount of radioactivity was quantified with a γ-counter in the soluble and nonsoluble TCA fractions of the supernatant and cell lysate. The total amount of endocytosed α2-macroglobulin was calculated by adding the radioactivity counted in these three fractions. No radioactivity was detected in the nonprecipitable, TCA fraction obtained from the cell lysate.

RESULTS

Truncated BBMI Proteins Were Recovered in Fractions Enriched in Membrane Vesicles and Codistributed with Internalized Ligands. We have prepared and isolated hepatoma cell lines producing chicken BBMI and two truncated proteins BBMI tail and BBMIΔ446 which are expected to be nonfunctional. BBMI tail (730–1040 aa) lacks the entire amino-terminal motor domain as well as two of its four putative calmodulin binding sites, whereas BBMIΔ446 (446–1040 aa) lacks the ATP binding site. The production of chicken BBMI and truncated variants in these cell lines was determined by immunoblotting using a monoclonal antibody directed against the carboxy-terminal domain of the chicken BBMI (CX-7 antibody) (33). In control cells that have been transfected with the expression vector alone, the CX-7 antibody did not detect any polypeptide corresponding to the electrophoretic migration of a myosin-I (Fig. 1*A*, lanes 1 and 5). In cells transfected with the cDNAs encoding BBMI, BBMIΔ446, and BBMI tail, proteins with an apparent molecular weight of 116 kDa, 74 kDa, and 31 kDa, respectively, were detected (Fig. 1*A*, lanes 2–4). Their apparent molecular weights on SDS/PAGE were compatible with the molecular weights calculated from the chicken BBMI sequence. BBMI and truncated BBMI were also detected on membrane fractions isolated from a post-

Panel A

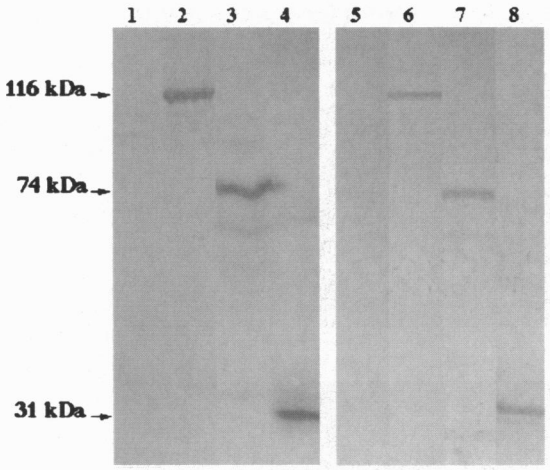

Panel B

	Cells	BBMI (7A)	IκB
Total cell homogenate	Mock	below the detection level	1
	BBMI	1	0,5
	BBMIΔ446	1	1
	Tail	1	0,75
membrane fractions	Mock	below the detection level	below the detection level
	BBMI	1,6	below the detection level
	BBMIΔ446	0,75	below the detection level
	Tail	1	below the detection level

FIG. 1. Immunoblot analysis and estimation of the amount of BBMI, and the truncated variants in cell homogenates and membrane fractions. (*A*) Immunoblot analysis. Proteins from cell homogenates, (lane 1–4) and from membrane fractions prepared as described (lane 5–8) were separated by SDS/7% PAGE, electrotransferred to nitrocellulose, and immunolabeled with the CX-7 antibody. The same amount of proteins from the different cell homogenates or membrane fractions were analyzed. Lanes 1 and 5 represent cell homogenate and membrane fraction from control cells, lanes 2 and 6 are cell homogenate and membrane fraction from cells producing BBMI, lanes 3 and 7 are cell homogenate and membrane fraction from cells producing BBMIΔ446, and lanes 4 and 8 are cell homogenate and membrane fraction from cells producing the BBMI tail. (*B*) Comparison of the amounts of BBMI, truncated variants, and IκBα in the membrane fractions with the amounts of these proteins in the total cell homogenates. The amounts of total proteins have been estimated on protein profiles stained with Ponceau S before the immunodetection, whereas BBMI, truncated variants, and IκBα have been estimated after immunodetection with the CX-7 antibody in the case of BBMI and the truncated variants and with a monoclonal antibody (42) in the case of IκBα by scanning densitometry, using the Bio profil system (Vilber Lourmat, Marne la Vallee, France). The amounts of BBMI and the truncated variants were normalized to the total amount of protein loaded and the total amount of BBMI or truncated variants detected in total cell homogenates. The amount of IκBα was normalized to the total amount of protein and to the amount of IκBα detected in the total cell homogenate of control cells.

nuclear supernatant by flotation on a sucrose gradient at a sucrose density of 35% (Fig. 1*A*, lanes 3–8). Similar amounts of these proteins were quantified in the membrane fraction and total cell homogenate whereas cytosolic proteins such as IκBα were easily monitored in the total cell homogenate but below the detection level in the membrane fractions (Fig. 1*B*).

Immunofluorescence labeling of cells producing BBMI using the CX-7 antibody showed a diffuse staining pattern and a recruitment of BBMI near the plasma membrane in lamellipodia (Fig. 2*A*). In these regions, BBMI was codistributed with some of the cortical actin filaments (Fig. 2*A*, *1* versus *2*, see arrows). BBMIΔ446 and BBMI tail was never found in lamellipodia. They were rather diffusely distributed throughout the cytoplasm and codistributed with cytoplasmic punctate structures (Fig. 2*B*). No significant modification of the organization of actin filaments can be detected at the optical level in cells producing BBMI as well as cells producing the truncated variants (Fig. 2*C*). The distribution of the cytoplasmic structures labeled with the CX-7 antibody was compared in cells producing BBMIΔ446 or BBMI tail with the distribution of organelles such as endoplasmic reticulum, Golgi apparatus, or endocytic compartments using the CLSM. They were not codistributed with endoplasmic reticulum and Golgi apparatus, but some of them were codistributed with discrete cytoplasmic structures containing fluorescent α2-macroglobulin internalized for 30 min. (Fig. 2*B*, *1* and *4* versus *2* and *5* and *3* and *6*, see arrows). Similarly, some of them were codistributed with the vesicular structures positive for endocytosed transferrin (data not shown). Because we have never been able to detect codistribution of the variants with ligand internalized for 5 min or with cathepsin D, we assume that the punctate structures codistributing with the variants do not correspond to early endosomes or lysosomes but rather to the distal compartment of the recycling pathway of the transferrin and late endosomes containing α2-macroglobulin.

Production of the Truncated BBMI Proteins Affects the Distribution of the Internalized Ligands and the Acidic Compartment. Within 5 min, ligands were mainly internalized in early endosomes located at the cell periphery in control cells as well as in cells producing the chicken BBMI or its truncated variants (data not shown). After 30 min of internalization, transferrin was predominantly distributed at one pole of the nucleus in control cells (Fig. 3 *A* and *B*) as previously shown. Transferrin internalized in the same conditions was also concentrated in the vicinity of the nucleus in cells producing BBMI (Fig. 3 *C* and *D*). In contrast, transferrin was dispersed throughout the cytoplasm in cells producing the truncated BBMI variants (Fig. 3 *E*, *F* and *G*, *H*). Similarly α2-macroglobulin internalized for 30 min was concentrated in the vicinity of the nucleus in control cells and cells producing BBMI, whereas it was dispersed in the cytoplasm of cells producing the truncated variants (data not shown). The altered distribution of these ligands was observed in all cellular clones producing the truncated variants and in HeLa cells transiently transfected with the same constructs encoding the truncated variants.

To determine whether the dispersion of the ligands after 30 min of internalization in cells producing truncated variants was due to an inhibition in the transfer of endocytosed ligands to the endocytic compartments in a juxtanuclear position and/or whether it was due to a disorganization of these late endocytic compartments, we analyzed the distribution of the acidic compartment. In control cells and in cells producing the wild-type BBMI protein, the acidic compartment labeled with acridine orange was seen as a juxtanuclear "cap" with a few vesicular profiles (Fig. 4 *A* and *C*). In cells producing BBMI-truncated variants, however, these acidic structures appeared fragmented into numerous vesicles of various size and scattered throughout the cytoplasm (Fig. 4 *B* and *D*).

Production of the Truncated BBMI Proteins Affects the Degradation of α2-Macroglobulin. We next examined whether these structural modifications of the endocytic compartments impaired their function. The number of receptors per cell for each ligand was similar in control cells and cells producing BBMI and the truncated variants. More than 85% of transferrin bound at the cells surface at 37°C were internalized

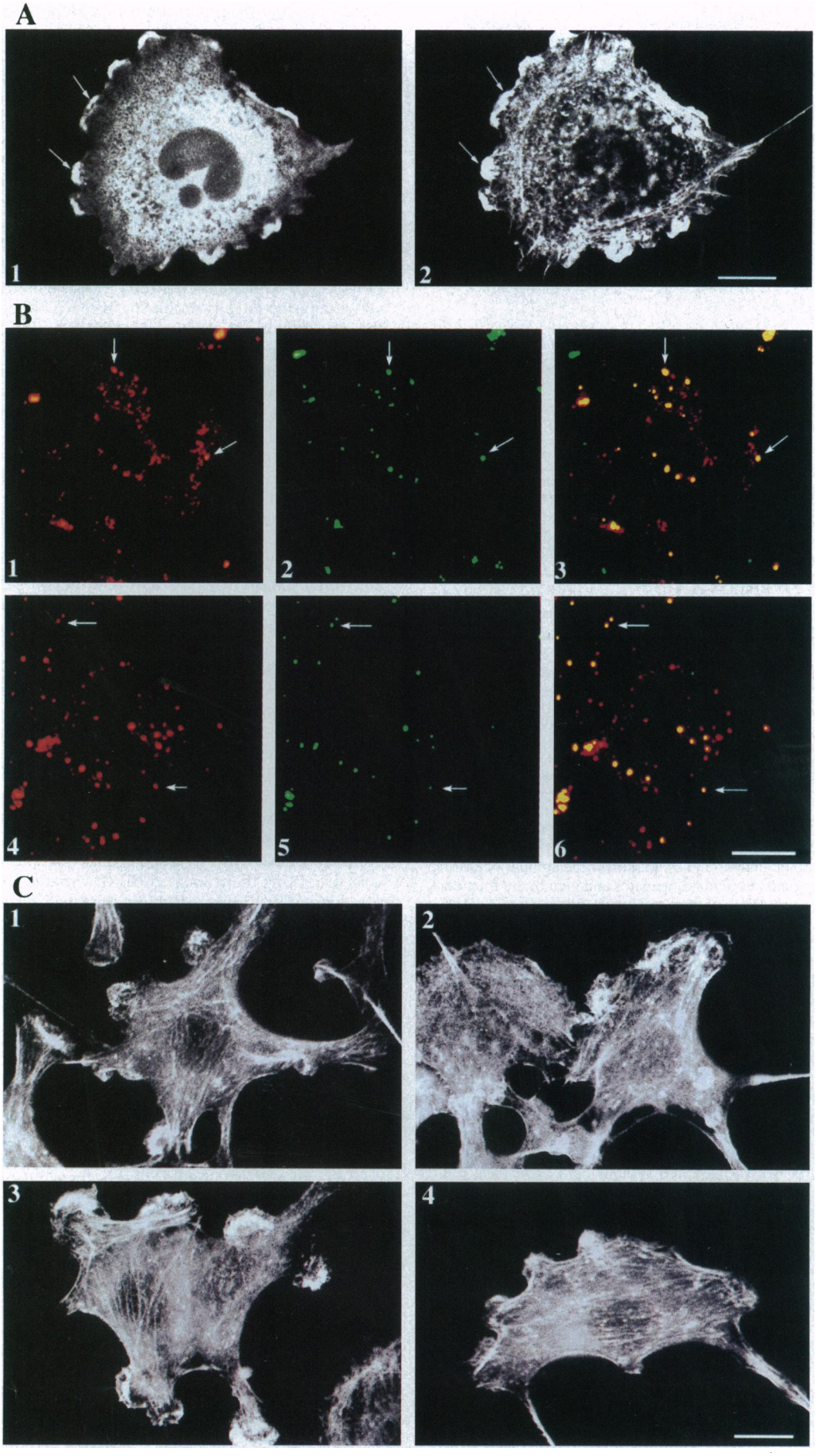

Fig. 2. (*Legend appears on the opposite page.*)

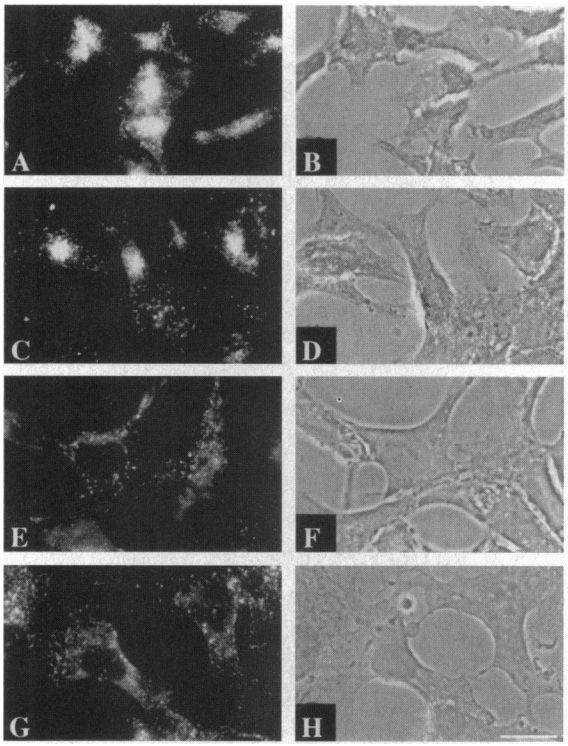

FIG. 3. Production of BBMI-truncated variants impairs the distribution of transferrin. The distribution of rhodamine conjugated transferrin (*A*, *C*, *E*, and *G*), internalized for 30 min at 37°C, was analyzed with an Axiophot microscope in cells producing BBMI (*C* and *D*), BBMIΔ446 (*E* and *F*), the BBMI tail (*G* and *H*), and in control cells (*A* and *B*). To visualize the cell margins, the cells were examined by phase contrast microscopy (*B*, *D*, *F*, and *H*). (Bar = 4 μm.)

within 20 min in control cells, cells producing BBMI, and cells producing the truncated variants. Furthermore 80% of the transferrin internalized were recycled within 20 min in control cells as in cells producing BBMI or the truncated variants. In contrast, the rate of α2-macroglobulin degradation decreased in 1 h, up to 40% in cells producing BBMIΔ446 and up to 15% in cell producing BBMI, but increased up to 35% in cells producing the tail protein (Fig. 5).

DISCUSSION

The Amino-Terminal Sequence Containing the ATP Binding Site Is Required for the Codistribution of BBMI with Cell Surface Structures Containing Actin. As predicted by the primary structure and as previously shown for membrane fraction derived from intestinal cells, the entire BBMI protein and the proteins truncated in the motor domain were detected in association with membrane fraction derived from hepatoma (37). It is likely that the absence of enrichment for BBMI or the truncated BBMI in the *bona fide* membrane fraction is due to a soluble pool that could account also for the cytoplasmic diffuse staining observed for these proteins by immunofluorescence.

Chicken BBMI produced in the hepatoma cell line (BWTG3) was codistributed with cortical actin cytoskeleton in lamellipodia,

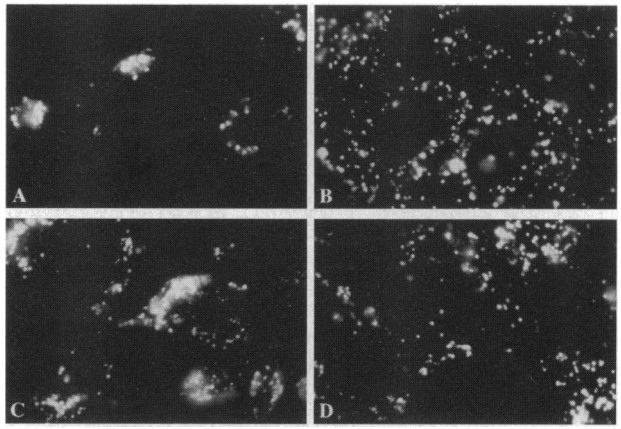

FIG. 4. Production of BBMI-truncated variants impairs the distribution of the acidic compartments. Acidic compartments was visualized in control cells (*A*), cells producing BBMI (*C*), BBMIΔ446 (*D*), and BBMI tail (*B*) by labeling them with acridine orange after sodium butyrate treatment. (Bar = 2 μm.)

suggesting its preferential targeting in a nonpolarized cell into cell surface structures enriched in actin microfilaments. A similar distribution has already been described in fibroblasts labeled with specific antibodies directed against BBMI and another member of the myosin-I family, suggesting that proteins immunologically related to BBMI can be detected in lamellipodia (22, 38). Furthermore, microinjected or recombinant chicken BBMI have been found located in the lamellipodia of Cos or 3T3 cells (25, 39). In contrast, the truncated proteins were found associated with punctate structures that codistributed to a certain extent with ligands internalized for 30 min. Thus, although the truncated BBMI proteins are still able to bind membrane fractions as predicted by their primary structure, their cytoplasmic distribution indicates that the amino-terminal sequence containing the ATP binding site is required for the codistribution of BBMI with cell surface structures containing actin.

BBMI Truncated Variants Have Dominant Effects on the Sorting of α2-Macroglobulin to the Degradative Compartment. The truncated BBMI proteins were found to affect the distribution of compartments containing the ligands internalized for 30 min and the acidic compartments. It is unlikely that truncated BBMI proteins affect the endosomal dynamic through a disorganization of actin filaments. Indeed, we have observed a similar distribution of the actin filaments in control cells and in cells producing truncated variants. We cannot completely ruled out that the production of truncated BBMI proteins could modify the localization and the size of the internal pool of calmodulin and thereby affect the endocytic process. However, the binding *in vitro* of BBMIΔ446 but not the tail to calmodulin (E.C., unpublished data) together with the partial codistribution of the truncated BBMI variants with the endocytic compartment are in favor of a direct effect of the truncated variants on the endocytic pathway.

The accumulation of the truncated proteins with dispersed endocytic compartments may reflect their inability under physiological conditions to move or to anchor these compart-

FIG. 2 (*legend from previous page*). Cellular distribution of BBMI, the truncated variants, and the actin filaments in the hepatoma cell lines. (*A*) Codistribution of BBMI with actin filaments in cells producing BBMI. The distribution of BBMI was analyzed as described with the CX-7 antibody (*1*) and the distribution of actin filaments with rhodamine-coupled phalloidin (*2*). Arrows indicate codistribution of BBMI with actin filaments from the cortical cytoskeleton. (Bar = 2 μm.) (*B*) Codistribution of BBMIΔ446 and BBMI tail with α2-macroglobulin. α2-Macroglobulin was internalized 30 min at 37°C as described. After fixation and permeabilization, cells were immunolabeled with the CX-7 and fluorescein anti-mouse antibodies. The distribution of BBMIΔ446 (*1*), BBMI tail (*4*), and the distribution of α2-macroglobulin in the corresponding cells (*2* and *5*), respectively, were analyzed by CLSM. Micrographs show sections of 0.5 mm through the nucleus. The combinations of *1* with *2*, and *4* with *5* are shown in *3* and *6*, respectively. The codistribution of the truncated variants and α2-macroglobulin in *3* and *6* is shown in yellow, whereas other structures remained in green or in red. Almost all the punctate structures corresponding to endocytosed α2-macroglobulin with an intensity of fluorescence higher than 40 arbitrary units (scale 0–255) are codistributed with the truncated variants (see arrows). (Bar = 5 μm.) (*C*) Cellular distribution of actin filaments in the hepatoma cell lines producing BBMI or the truncated variants. Actin filaments were detected with rhodamine-coupled phalloidin in control cells (*1*), cells producing BBMI (*2*), BBMIΔ446 (*3*), and the tail (*4*).

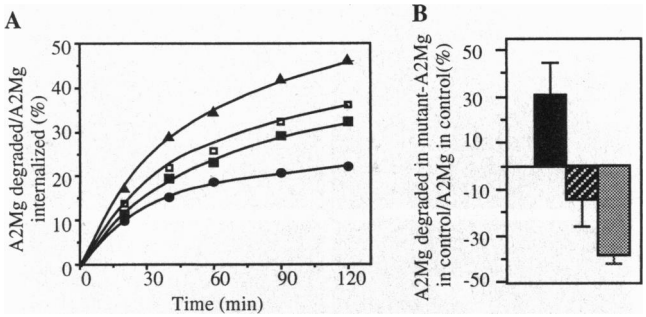

FIG. 5. Production of BBMI and its truncated variants modifies the rate of α2-macroglobulin degradation. ^{125}I-labeled α2-macroglobulin (10 μg/ml) was internalized for 30 min in control cells and in cells producing BBMI or its truncated variants at 37°C. Then cells were rinsed free of ligands and reincubated at 37°C for specified times. The amount of radioactivity contained in the TCA-soluble fractions corresponding to the degraded α2-macroglobulin was normalized to the total amount of endocytosed α2-macroglobulin. (*A*) Mean (standard errors are <5%) of four [for cells producing BBMIΔ446; (●)], five [for cells producing tail (▲)], or six [for control cells (□) and cells producing BBMI (■)] experiments in which the rates of α2-macroglobulin degradation were plotted at specified times. (*B*) Decrease or increase of α2-macroglobulin degraded in cells producing BBMI and its truncated variants over the α2-macroglobulin degraded in control cells at 1 h. The ratio of α2-macroglobulin degraded is increased up to 45% in cells producing the BBMI tail ($P < 0.005$, paired Student's *t* test) and is decreased up to 38.2% and 25% in cells producing BBMIΔ446 ($P < 0.007$, paired Student's *t* test) and BBMI ($P < 0.001$, paired Student's *t* test), respectively. These increases and decreases remain stable during the time of follow up.

ments transiently on actin filaments. Although the two truncated variants have a dominant effect on the rate of the delivery of ligands to the degradative compartments, the production of BBMIΔ446 slows down the rate of the degradation of α2-macroglobulin, whereas the production of the tail increases this rate. According to these data, an attractive working hypothesis would be that BBMIΔ446, lacking the ATP binding site, would bridge endocytic compartments to actin microfilaments but would be unable to exert tensions or movement of these compartments along actin filaments in an ATP-dependent manner. In contrast, the tail variant, lacking the ATP and the actin binding sites, would be unable to link endocytic compartments to actin filaments. In agreement with this hypothesis, BBMIΔ446 would slow down the delivery of ligands to the degradative compartment, whereas the tail variant would increase the fusion events between the endocytic compartments and the degradative compartment. A detailed analysis at the electron microscope level of the organization of the endocytic compartment associated with the truncated BBMI proteins is currently under investigation to test this hypothesis.

In the view of our observations and recent reports indicating that actin filaments were required for the delivery of ligands such as α2-macroglobulin and ricin to the degradative compartment, we propose that an endogenous myosin-I related to BBMI binds transiently the juxtanuclear endosomes on actin filaments and thereby regulates the delivery of ligands to the degradative compartments (40, 41). Antibody directed against the head domain of chicken BBMI (CX-1; ref. 33) allowed us to detect three polypeptides in the BWTG3 hepatoma cell line, whose size is in agreement with the size of members of the myosin-I family (E.C., unpublished data). However, further analysis is necessary to demonstrate that these immunologically related proteins are indeed endogenous myosins-I associated with the endocytic pathway. According to this model, calmodulin that regulates the binding *in vitro* of myosin-I to liposomes or membranes vesicles might control this step of endocytosis by controlling the activity of the myosin-I. Wild-type BBMI, which might have a similar function to the putative endogenous myosin-I, might increase to some extent the "clamp activity" of the putative endogenous myosin-I, whereas the two variants might compete with the endogenous myosin-I to bind transiently the juxtanuclear endosomes on actin filaments and thereby inhibit its function. Altogether, these data suggest the involvement of an acto–myosin-driven mechanism for maintaining the distribution the endocytic compartments in a juxtanuclear position and for controlling the rate of delivery of the ligands to the degradative compartments.

We wish to thank R. Hellio for his contribution and helpful advise for confocal microscopy, Drs. M. Mooseker (Yale University), R. Hay (University of Oxford), and K. Wood (University of St. Andrews, Scotland) for their generous gifts of antibodies and Dr. M. Weiss (Pasteur Institute) for the generous gift of the BWGT3 hepatoma cell line. Thanks are also due to Dr. R. Golsteyn for critically reading the manuscript and for his constructive comments. This work was supported by grants from the Association pour la Recherche Médicale sur le Cancer (ARC 6379), The Ligue Nationale Française contre le Cancer, and the Human Capital and Mobility (European Community Grant CHRX CT 94–0430). A.D. received a fellowship from the Pasteur Institute.

1. Barylko, B., Wagner, M. C., Reizes, O. & Albanesi, J. P. (1992) *Proc. Natl. Acad. Sci. USA* **89,** 490–494.
2. Bähler, M., Kroschewski, R., Stöffler, H. & Behrmann, T. (1994) *J. Cell Biol.* **126,** 375–389.
3. Colluccio, M. L. & Conaty, C. (1993) *Cell Motil. Cytoskeleton* **24,** 189–199.
4. Garcia, A., Coudrier, E., Carboni, J., Anderson, J., Vandekerkhove, J., Mooseker, M., Louvard, D. & Arpin, M. (1989) *J. Cell Biol.* **109,** 2895–2903.
5. Mooseker, M. S., Wolenski, J. S., Coleman, T. R., Hayden, M. B., Cheney, R. E., Espraefico, E., Heintzelman, M. B. & Peterson, M. D. (1991) *Curr. Top. Membr.* **38,** 31–55.
6. Pollard, T. D., Doberstein, S. K. & Zot, H. G. (1991) *Annu. Rev. Physiol.* **53,** 653–681.
7. Ruppert, C., Kroschewski, R. & Bähler, M. (1993) *J. Cell Biol.* **120,** 1393–1403.
8. Sheer, E. H., Joyce, M. P. & Greene, L. A. (1993) *J. Cell Biol.* **120,** 1405–1416.
9. Hayden, S. M., Wolenski, J. S. & Mooseker, M. S. (1990) *J. Cell Biol.* **111,** 443–451.
10. Cheney, R., Riley, M. A. & Mooseker, M. S. (1993) *Cell Motil. Cytoskeleton* **24,** 215–223.
11. Baines, I., C. & Korn, E. D. (1990) *J. Cell Biol.* **111,** 1895–1904.
12. Baines, I. C., Brzeska, H. & Korn, E. D. (1992) *J. Cell Biol.* **119,** 1193–1203.
13. Baines, I. C., Corigliano-Murphy, A. & Korn, E. D. (1995) *J. Cell Biol.* **130,** 591–603.
14. Bement, W. M., Hasson, T., Wirth, J. A., Cheney, R. E. & Mooseker, M. S. (1994) *Proc. Natl. Acad. Sci. USA* **91,** 6549–6553.
15. Doberstein, S. K., Baines, I. C., Wiegand, G., Korn, E. D. & Pollard, T. D. (1993) *Nature (London)* **365,** 841–843.
16. McGoldrick, C. A., Gruver, C. & May, G. S. (1995) *J. Cell Biol.* **128,** 577–587.
17. Titus, M., A., Wessels, D., Spudich, J. A. & Soll, D. (1993) *Mol. Biol. Cell* **4,** 233–246.
18. Novak, K. D., Peterson, M. D., Reedy, M. C. & Titus, M. A. (1995) *J. Cell Biol.* **131,** 1205–1221.
19. Bikle, D., Munson, S. & Mancianti, M. L. (1991) *Gastroenterology* **100,** 395–402.
20. Coudrier, E., Reggio, H. & Louvard, D. (1981) *J. Mol. Biol.* **152,** 49–66.
21. Drenckhahn, D. & Dermietzel, R. (1988) *J. Cell Biol.* **107,** 1037–1048.
22. Wagner, M. C., Barylko, B. & Albanesi, J. P. (1992) *J. Cell Biol.* **119,** 163–170.
23. Colluccio, L. M. & Bretcher, A. (1989) *J. Cell Biol.* **108,** 495–502.
24. Matsudaira, P. T. & Burgess, D. R. (1979) *J. Cell Biol.* **83,** 667–673.
25. Collins, K. & Matsudaira, P. T. (1995) *Cell Motil. Cytoskeleton* **32,** 151–161.
26. Hoshimaru, M. & Nakanishi, S. (1987) *J. Biol. Chem.* **262,** 14625–14632.
27. Szpirer, C. & Szpirer, J. (1975) *Differentiation* **4,** 85–91.
28. Felger, P. L., Gadek, T. R., Holm, M., Roman, R., Chan, H. W., Wenz, M., Nortrop, J. P., Ringold, G. M. & Danielsen, M. (1987) *Proc. Natl. Acad. Sci. USA* **84,** 7413 - 7417.
29. Gorman, C. M. & Howard, B. H. (1983) *Nucleic Acids Res.* **11,** 7631–7648.
30. Brandzaeg, P. (1973) *Scand. J. Immunol.* **2,** 273–290.
31. Maxfield, F. R., Schlessinger, J., Shechter, Y., Pastan, I. & Willingham, M. C. (1978) *Cell* **14,** 805–810.
32. Mosher, D. F., Saksela, O. & Vaheri, A. (1977) *J. Clin. Invest.* **60,** 1036–1045.
33. Carboni, J. M., Conzelman, K. A., Adams, R. A., Kaiser, D. A., Pollard, T. D. & Mooseker, M. S. (1988) *J. Cell Biol.* **107,** 1749–1757.
34. Hopkins, C. R. (1983) *Cell* **35,** 321–330.
35. Hopkins, C. R., Gibson, A., Shipman, M., Strickland, D. K. & Trowbridge, I. S. (1994) *J. Cell Biol.* **125,** 1265–1274.
36. Matteoni, R. & Kreis, T. E. (1987) *J. Cell Biol.* **105,** 1253–1265.
37. Mooseker, M. S., Conzelman, K. A., Coleman, T. R., Heuzer, J. E. & Sheetz, M. P. (1989) *J. Cell Biol.* **109,** 1153–1161.
38. Conrad, P. A., Giuliano, K. A., Fisher, G., Collins, K., Matsudaira, P., T. & Taylor, D. L. (1993) *J. Cell Biol.* **120,** 1381–1391.
39. Footer, M. & Brestcher, A. (1994) *J. Cell Sci.* **107,** 1623–1631.
40. Van Deurs, B., Holm, P. K., Kayser, L. & Sandvig, K. (1995) *Eur. J. Cell Biol.* **66,** 309–323.
41. Durrbach, A., Louvard, D., &Coudrier, E. (1996) *J. Cell Sci.* **109,** 457–465.
42. Jaffray, E., Wood, K. M. & Hay, R. T. (1995) *Mol. Cell. Biol.* **15,** 2166–2172.